

Heterolysis of H–X Bonds by Pentamethylcyclopentadienyl–Aminoborole Complexes of Zirconium and Hafnium

Andrew F. Kiely, Cory M. Nelson, Antonio Pastor, Lawrence M. Henling, Michael W. Day, and John E. Bercaw*

Arnold and Mabel Beckman Laboratories of Chemical Synthesis, California Institute of Technology, Pasadena, California 91125

Received October 27, 1997

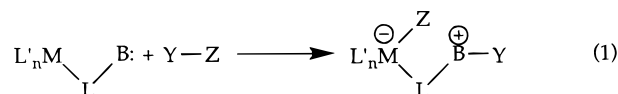
The pentamethylcyclopentadienyl–aminoborole chloro complexes $\text{Cp}^*\{\eta^5\text{-C}_4\text{H}_4\text{BN}(\text{CHMe}_2)_2\}\text{MCl}\cdot\text{LiCl}$ ($\text{Cp}^* = (\eta^5\text{-C}_5\text{Me}_5)$; $\text{M} = \text{Zr, Hf}$) heterolytically cleave H–X bonds to form $\text{Cp}^*\{\eta^5\text{-C}_4\text{H}_4\text{BNH}(\text{CHMe}_2)_2\}\text{MCl}(\text{X})$ ($\text{X} = \text{OR, SR, C}\equiv\text{CR}$). Control experiments using deuterium-labeled substrates show heterolysis occurs with no incorporation of deuterium into the 2,5 positions of the borole heterocycle. $\text{Cp}^*\{\eta^5\text{-C}_4\text{H}_4\text{BNH}(\text{CHMe}_2)_2\}\text{Hf}(\text{C}\equiv\text{CSiMe}_3)_2$ is prepared from $\text{Cp}^*\{\eta^5\text{-C}_4\text{H}_4\text{BN}(\text{CHMe}_2)_2\}\text{Hf}(\eta^3\text{-C}_3\text{H}_5)$ and 2 equiv of (trimethylsilyl)acetylene. Treatment of $\text{Cp}^*\{\eta^5\text{-C}_4\text{H}_4\text{BN}(\text{CHMe}_2)_2\}\text{MCl}\cdot\text{LiCl}$ ($\text{M} = \text{Zr, Hf}$) with donor ligands L yields the LiCl-free complexes $\text{Cp}^*\{\eta^5\text{-C}_4\text{H}_4\text{BN}(\text{CHMe}_2)_2\}\text{MCl}(\text{L})$ ($\text{M} = \text{Zr, L} = \text{NMe}_2\text{H}$; $\text{M} = \text{Hf, L} = \text{PMe}_3$). $\text{Cp}^*\{\eta^5\text{-C}_4\text{H}_4\text{BN}(\text{CHMe}_2)_2\}\text{HfCl}(\text{PMe}_3)$ reacts with (trimethylsilyl)acetylene with loss of $\text{HN}(\text{CHMe}_2)_2$ to form $\text{Cp}^*\{\eta^5\text{-C}_4\text{H}_4\text{B}(\text{C}\equiv\text{CSiMe}_3)\}\text{HfCl}(\text{PMe}_3)$, resulting from formal migration of acetylde from hafnium to boron. X-ray structure determinations of $\text{Cp}^*\{\eta^5\text{-C}_4\text{H}_4\text{BNH}(\text{CHMe}_2)_2\}\text{HfCl}(\text{C}\equiv\text{CSiMe}_3)$, $\text{Cp}^*\{\eta^5\text{-C}_4\text{H}_4\text{BN}(\text{CHMe}_2)_2\}\text{HfCl}(\text{PMe}_3)$, and $\text{Cp}^*\{\eta^5\text{-C}_4\text{H}_4\text{B}(\text{C}\equiv\text{CSiMe}_3)\}\text{HfCl}(\text{PMe}_3)$ are reported.

Introduction

Transition-metal complexes having ligands with donor groups have been widely employed. The donor group may (a) simply function as a ligand for another transition-metal center (e.g., as for ferrocenyl phosphines),¹ (b) bind to the otherwise coordinatively unsaturated transition- or main-group-metal center in a chelating fashion, or (c) serve as a carrier for polar species (e.g., NaH, LiMe) in nonpolar solvents.² When chelation and bridging interactions are discouraged, the Lewis basic site may undergo the usual protonation and alkylation reactions;³ however, in cases where the lone electron pair of the Lewis base is in conjugation with the ancillary ligand, it may be significantly less nucleophilic. For example, Boche and co-workers noted that the amino groups of bis(dimethylamino)titanocene dichloride are not readily alkylated, consistent with the strong interaction between the amino group and the cyclopentadienyl ligand.⁴ Such a π -interaction between the

substituents and ligand is frequently observed for heterocyclic ligands such as aminoboratabenzenes and aminoboroles.⁵

When the complex is deliberately designed to avoid π conjugation from the basic site into the ligand, the two sites may work in concert to heterolyze σ bonds (eq 1). Such heterolytic reactivity would, thus, be analogous



to the now well-established 1,2-addition of H–X bonds across early-transition-metal-to-heteroatom bonds, demonstrated for metal imido,⁶ phosphinidene,⁷ oxo,⁸ or sulfido⁹ bonds (eq 2). One may view the two processes

(1) (a) Cullen, W. R.; Woollins, J. D. *Coord. Chem. Rev.* **1982**, *39*, 1 and references therein. (b) Hayashi, T.; Kumada, M. *Acc. Chem. Res.* **1982**, *15*, 395. (c) Hayashi, T.; Konishi, M.; Ito, H.; Kumada, M. *J. Am. Chem. Soc.* **1984**, *106*, 4962.

(2) (a) Jacoby, D.; Floriani, C.; Chiesi-Villa, A.; Rizzoli, C. *J. Am. Chem. Soc.* **1993**, *115*, 3595. (b) Jacoby, D.; Isoz, S.; Floriani, C.; Chiesi-Villa, A.; Rizzoli, C. *J. Am. Chem. Soc.* **1995**, *117*, 2805. (c) Gallo, E.; Solari, E.; Floriani, C.; Chiesi-Villa, A.; Rizzoli, C. *Organometallics* **1995**, *14*, 2156. (d) De Angelis, S.; Solari, E.; Floriani, C.; Chiesi-Villa, A.; Rizzoli, C. *Organometallics* **1995**, *14*, 4505. (e) Jacoby, D.; Isoz, S.; Floriani, C.; Schenk, K.; Chiesi-Villa, A.; Rizzoli, C. *Organometallics* **1995**, *14*, 4816.

(3) (a) Jutzi, P.; Siemeling, U. *J. Organomet. Chem.* **1995**, *500*, 175 and references therein. (b) Jutzi, P.; Dahlhaus, J. *Coord. Chem. Rev.* **1994**, *137*, 179 and references therein.

(4) Stahl, K.-P.; Boche, G.; Massa, W. *J. Organomet. Chem.* **1984**, *277*, 113.

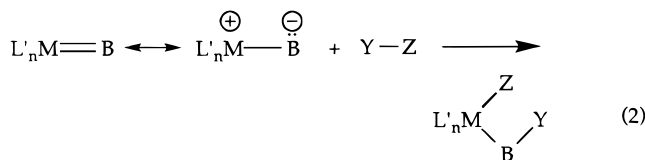
(5) Boratabenzenes, see: (a) Herberich, G. E.; Ohst, H. *Adv. Organomet. Chem.* **1986**, *25*, 199 and references therein. (b) Herberich, G. E.; Schmidt, B.; Englert, U.; Wagner, T. *Organometallics* **1993**, *12*, 2891. (c) Herberich, G. E.; Schmidt, B.; Englert, U. *Organometallics* **1995**, *14*, 471. (d) Ashe, A. J.; Kampf, J. W.; Muller, C.; Schneider, M. *Organometallics* **1996**, *15*, 387. Boroles, see: (e) Herberich, G. E.; Hostalek, M.; Laven, R.; Boese, R. *Angew. Chem., Int. Ed. Engl.* **1990**, *29*, 317. (f) Herberich, G. E.; Hessner, B.; Ohst, H.; Rapp, I. A. *J. Organomet. Chem.* **1988**, *348*, 305. (g) Herberich, G. E.; Negele, M.; Ohst, H. *Chem. Ber.* **1991**, *124*, 25. (h) Bazan, G. C.; Donnelly, S. J.; Rodriguez, G. *J. Am. Chem. Soc.* **1995**, *117*, 2671.

(6) (a) Schaller, C. P.; Cummins, C. C.; Wolczanski, P. T. *J. Am. Chem. Soc.* **1996**, *118*, 591 and references therein. (b) Lee, S. Y.; Bergman, R. G. *J. Am. Chem. Soc.* **1995**, *117*, 5877 and references therein.

(7) Breen, T. L.; Stephan, D. W. *J. Am. Chem. Soc.* **1995**, *117*, 11914 and references therein.

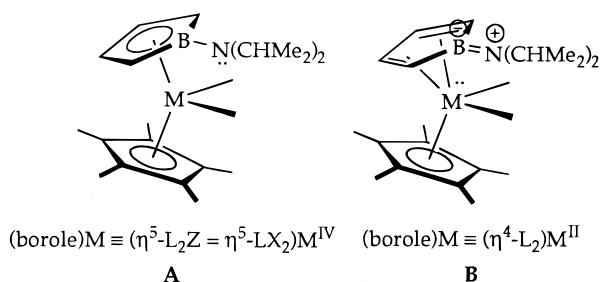
(8) (a) Howard, W. A.; Waters, M.; Parkin, G. *J. Am. Chem. Soc.* **1993**, *115*, 4917. (b) Smith, M. R.; Matsunaga, P. T.; Andersen, R. A. *J. Am. Chem. Soc.* **1993**, *115*, 7049.

(9) Howard, W. A.; Parkin, G. *J. Am. Chem. Soc.* **1994**, *116*, 606.

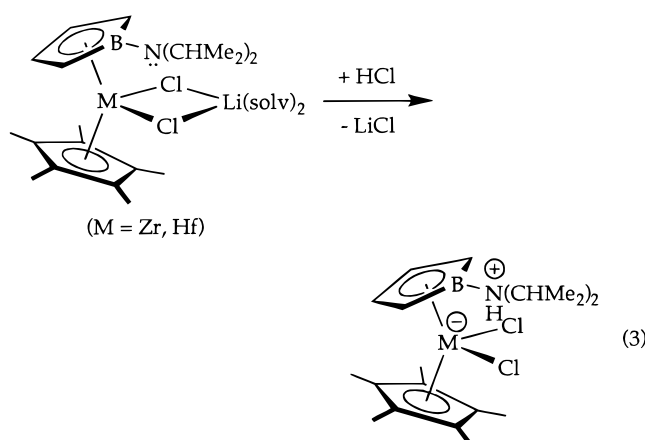


as closely related, with the Lewis base in the former effectively extended from the electrophilic metal center by the intervening ligand atoms.

Recently, we have been investigating mixed aminoborole–pentamethylcyclopentadienyl derivatives of zirconium and hafnium as metallocene analogues.¹⁰ Aside from their similarity to d⁰ metallocenes, these complexes proved to be amphoteric, possessing both electrophilic and nucleophilic sites of reactivity. Experimental evidence supports two contributing canonical forms (**A** and **B**). Since the early-transition-metal



center is relatively difficult to reduce from its highly favored tetravalent state, **A** is an important contributor and the lone electron pair remains localized on nitrogen, making it relatively basic. Thus, these complexes were prime candidates for promoting σ-bond heterolysis, as represented in eq 1. We have demonstrated that these complexes may heterolyze σ bonds with a trivial reaction of Cp*{η⁵-C₄H₄BN(CHMe₂)₂}MCl·LiCl(sol_v)₂ (M = Zr, Hf) with HCl, generating Cp*{η⁵-C₄H₄BNH(CHMe₂)₂}MCl₂ (eq 3).¹⁰

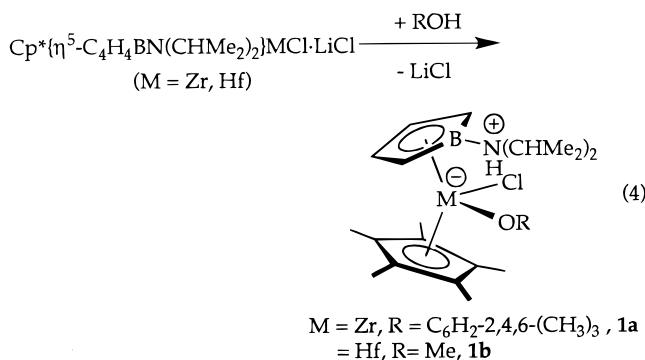


We now report reactions of Cp*{η⁵-C₄H₄BN(CHMe₂)₂}MCl·LiCl (M = Zr, Hf), Cp*{η⁵-C₄H₄BN(CHMe₂)₂}HfCl(PMe₃), and Cp*{η⁵-C₄H₄BN(CHMe₂)₂}Hf(η³-C₃H₅) with less readily heterolyzed H–X bonds of alcohols, thiols, and (trimethylsilyl)acetylene.

(10) (a) Quan, R. W.; Bazan, G. C.; Kiely, A. F.; Schaefer, W. P.; Bercaw, J. E. *J. Am. Chem. Soc.* **1994**, *116*, 4489. (b) Pastor, A.; Kiely, A. F.; Henling, L. M.; Day, M. W.; Bercaw, J. E. *J. Organomet. Chem.* **1997**, *528*, 65.

Results and Discussion

Treatment of Cp*{η⁵-C₄H₄BN(CHMe₂)₂}MCl·LiCl (M = Zr, Hf) with alcohols (HOR) results in the formation of Cp*{η⁵-C₄H₄BNH(CHMe₂)₂}MCl(OR) or a mixture of Cp*{η⁵-C₄H₄BNH(CHMe₂)₂}MCl(OR) and Cp*{η⁵-C₄H₄BNH(CHMe₂)₂}MCl₂. Thus, Cp*{η⁵-C₄H₄BN(CHMe₂)₂}ZrCl·LiCl reacts with 1 equiv of 2,4,6-trimethylphenol to yield exclusively the green complex **1a**, Cp*{η⁵-C₄H₄BNH(CHMe₂)₂}ZrCl(–OC₆H₂-2,4,6-(CH₃)₃), while Cp*{η⁵-C₄H₄BN(CHMe₂)₂}HfCl·LiCl reacts with 1 equiv of HOME to yield yellow Cp*{η⁵-C₄H₄BNH(CHMe₂)₂}HfCl(OMe), **1b**, and Cp*{η⁵-C₄H₄BNH(CHMe₂)₂}HfCl₂ in a 4:1 ratio. This ratio is increased when an excess of HOME is used, so that it is possible to isolate pure **1b** in good yield when 20 equiv of methanol is employed in the reaction (eq 4). Both **1a** and **1b** are soluble in

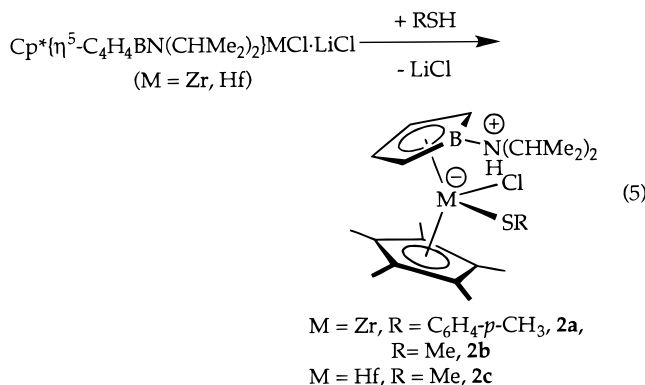


aliphatic hydrocarbons and display the expected C₁ symmetry in solution, with all four hydrogens of the borole and all four isopropyl methyl groups inequivalent in their ¹H NMR spectra.

The colors of **1a** and **1b** display the expected blue shift compared to the starting complexes. On the basis of our previous examination of the spectroscopy of these complexes, we have concluded that the HOMO is predominantly aminoborole-based and the LUMO is predominantly metal-based.^{10b} These compounds are intensely colored because of a strong LMCT transition which occurs in the visible region. In agreement with this assignment, protonation of the nitrogen of the aminoborole stabilizes the HOMO and, thus, leads to the observed increase in the energy of this transition.

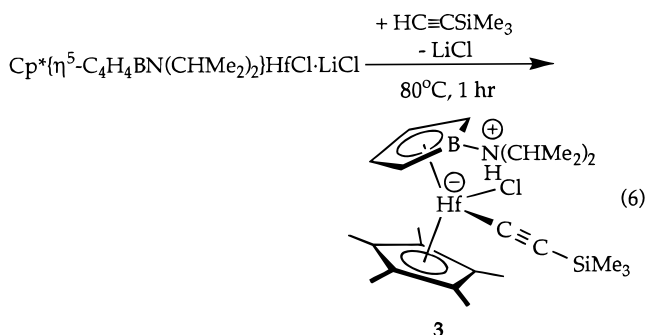
An NMR study of the formation of **1a** indicates that Cp*{η⁵-C₄H₄BNH(CHMe₂)₂}ZrCl₂ and (presumably) LiOC₆H₂-2,4,6-(CH₃)₃ are formed initially and that these species subsequently react more slowly to form **1a** and LiCl. It is possible that the role of excess alcohol in changing the product ratio is simply to solubilize the initially formed LiOR so that it may react further with the organometallic species.

In contrast to the mixtures of products obtained from the reaction between Cp*{η⁵-C₄H₄BN(CHMe₂)₂}MCl·LiCl (M = Zr, Hf) and alcohols, the reactions with thiols result exclusively in the formation of the thiolate derivatives Cp*{η⁵-C₄H₄BNH(CHMe₂)₂}MCl(SR) (M = Zr, R = C₆H₄-*p*-CH₃, **2a**, R = Me, **2b**; M = Hf, R = Me, **2c**) (eq 5). The yellow *p*-tolyl thiolate derivative **2a** and the orange-yellow methyl thiolate derivatives **2b** and **2c** are soluble in aromatic hydrocarbon solvents, and all three complexes display the expected C₁ symmetry in solution (see Experimental Section). The broad peak



in the ¹H NMR spectrum attributed to the N–H hydrogen is found at δ 6.4 for complex **2a**. This shift is similar to that found for complexes **1a** (δ 6.7) and **1b** (δ 6.5) as well as for Cp*{ η^5 -C₄H₄BNH(CHMe₂)₂}HfCl₂ (δ 6.4). The N–H resonance is found at somewhat lower field, δ ~7.5, for **2b** and **2c**.

The reaction between Cp*{ η^5 -C₄H₄BN(CHMe₂)₂}HfCl·LiCl and (trimethylsilyl)acetylene occurs under slightly more forcing conditions than those required for the reactions with alcohols and thiols (eq 6). As the



reaction proceeds, the mostly toluene-insoluble Cp*{ η^5 -C₄H₄BN(CHMe₂)₂}HfCl·LiCl complex gradually disappears, leaving a white solid (presumably LiCl) and an orange solution. Recrystallization of the crude product from hot heptane results in a ~65% yield of yellow crystalline **3**. ¹H NMR spectra for **3** are consistent with its formulation as a complex containing a σ -bonded acetylide and a protonated amino group. To verify the bonding in complex **3**, we undertook a single-crystal X-ray structure determination. An ORTEP plot with 30% displacement ellipsoids is shown in Figure 1, crystal data are listed in Table 1, and selected bond distances and angles are given in Table 2. Generally, the bond distances and angles are similar to those found in the structure of Cp*{ η^5 -C₄H₄BNH(CHMe₂)₂}HfCl₂.^{10a} In the structure determination, the amino hydrogen was located in the difference map, but this atom was set at a fixed distance of 0.95 Å and no parameters for it were refined. Additional support for the presence of a proton on the nitrogen comes from the B–N bond distance (1.571(8) vs 1.43 Å for Cp*{ η^5 -C₄H₄BN(CHMe₂)₂}HfCl·LiCl)¹⁰ and the nonplanar bond angles around the nitrogen (sum of angles = 344°). One difference between the structure of **3** and that of Cp*{ η^5 -C₄H₄BNH(CHMe₂)₂}HfCl₂ is that there is no evidence for an intramolecular hydrogen bond between the N–H moiety and the chloride ligand for **3**; rather, the NH moiety is positioned over the trimethylsilylacetylide ligand.

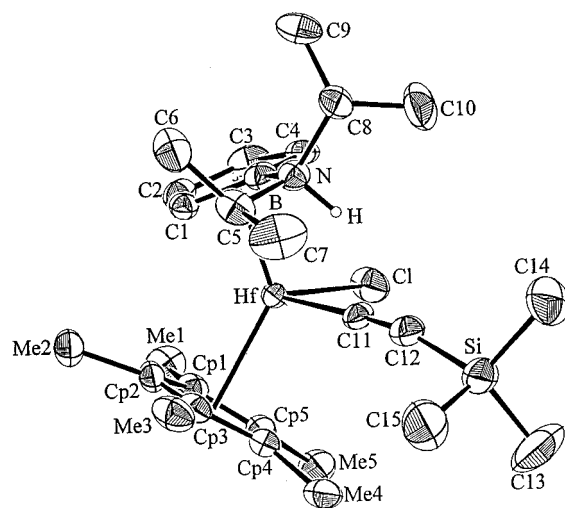


Figure 1. Drawing of Cp*{ η^5 -C₄H₄BNH(CHMe₂)₂}HfCl·LiCl (C≡CSiMe₃) (**3**) (30% ellipsoids).

Table 1. Crystal Data^a

	3	5b	6
formula	C ₂₅ H ₄₃ BCl- HfNSi	C ₂₃ H ₄₂ BCl- HfNP	C ₂₂ H ₃₇ BCl- HfPSi
mol wt	610.46	588.30	585.35
color	yellow	dark blue	orange
habit	lozenge	irregular	cluster
cryst size, mm	0.30 × 0.37 × 0.63	0.20 × 0.40 × 0.50	0.17 × 0.19 × 0.24
cryst syst	monoclinic	monoclinic	orthorhombic
space group	P2 ₁ /n (No. 14)	P2 ₁ (No. 4)	P2 ₁ 2 ₁ 2 ₁ (No. 19)
a, Å	8.237(2)	8.876(3)	12.168(4)
b, Å	12.210(3)	16.293(6)	13.651(4)
c, Å	29.204(5)	9.072(3)	15.692(5)
α, deg	90	90	90
β, deg	97.68(2)	96.34(2)	90
γ, deg	90	90	90
V, Å ³	2910.8(11)	1303.9(8)	2606.5(14)
Z	4	2	4
d _{calc} , g cm ⁻³	1.39	1.49	1.49
μ, cm ⁻¹	36.96	41.73	42.15
trans coeff	0.90, 1.10	0.75, 1.21	0.80, 1.28
decay, %	8.9		
2θ range, deg	3, 50	2, 50	2, 50
h min, max	-9, 9	0, 10	-14, 0
k min, max	0, 14	-19, 19	-16, 16
l min, max	-34, 34	-10, 10	-18, 0
no. of reflns	11 116	5222	8619
no. of indep. reflns	5128	4574	2601
GOF merge (mult.)	1.17 (5117)	1.54 (648)	1.81 (2360)
R(F)	0.048 ^b	0.034 ^c	0.036 ^b
R _w (F ²) ^d	0.062	0.063	0.064
GOF ^e	1.42	1.79	1.66
data, params	5128, 271	4574, 318	2601, 244
Δρ max, min, e Å ⁻³	0.63, -0.51	0.53, -0.45	2.31, -1.05

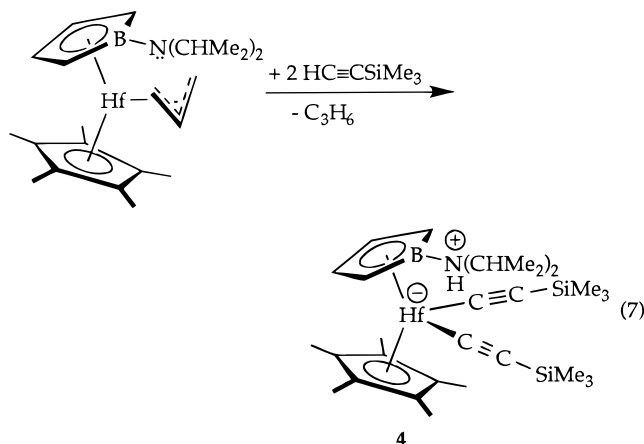
^a Nonius CAD-4 diffractometer, Mo Kα radiation, λ = 0.7107 Å, graphite monochromator, ω scans. ^b R(F) = Σ|F_c - F_o|/ΣF_o, F_o > 0. ^c R(F) = Σ||F_c| - |F_o||/Σ|F_o|. ^d R_w(F²) = [Σw(F_o² - F_c²)²]/Σw(F_o²)^{1/2}. ^e GOF = [Σw(F_o² - F_c²)²/(n - p)]^{1/2}.

Another important but somewhat puzzling difference between complex **3** and the HCl analogue is that complex **3** can only be prepared in noncoordinating solvents. Thus, in contrast to the synthesis of Cp*{ η^5 -C₄H₄BNH(CHMe₂)₂}HfCl₂, which is best carried out in THF, the synthesis of **3** must be carried out in toluene. No reaction is observed in THF even if the mixture is maintained at 80 °C for weeks.

Table 2. Selected Distances (Å) and Angles (deg) for Cp* $\{\eta^5\text{-C}_4\text{H}_4\text{BN}(\text{CHMe}_2)_2\}\text{HfCl}(\text{C}\equiv\text{CSiMe}_3)$ (3)

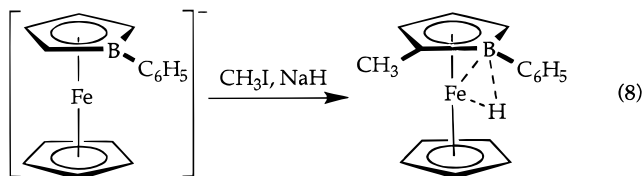
Hf–Cp* centroid	2.166	C3–C4	1.413(8)
Hf–Cl	2.432(2)	Si–C12	1.840(7)
Hf–C11	2.237(6)	N–H	0.95
C11–C12	1.196(8)	Hf–C1	2.472(5)
B–C1	1.482(8)	Hf–C2	2.388(6)
B–C4	1.506(8)	Hf–C3	2.446(6)
B–N	1.571(8)	Hf–C4	2.519(5)
C1–C2	1.426(7)	Hf–B	2.620(7)
C2–C3	1.393(8)		
Hf–C11–C12	173.9(5)	C8–N–B	117.6(4)
Cp*–Hf–centroid _B	133.7	C8–N–C5	113.5(4)
C5–N–B	112.7(4)	Σ –N	343.8°

We have also investigated the reactivity of Cp* $\{\eta^5\text{-C}_4\text{H}_4\text{BN}(\text{CHMe}_2)_2\}\text{Hf}(\eta^3\text{-C}_3\text{H}_5)$ toward (trimethylsilyl)acetylene. Treatment of Cp* $\{\eta^5\text{-C}_4\text{H}_4\text{BN}(\text{CHMe}_2)_2\}\text{Hf}(\eta^3\text{-C}_3\text{H}_5)$ with 2 equiv of (trimethylsilyl)acetylene results in the quantitative formation of orange-yellow Cp* $\{\eta^5\text{-C}_4\text{H}_4\text{BN}(\text{CHMe}_2)_2\}\text{Hf}(\text{C}\equiv\text{CSiMe}_3)_2$, **4**, and propene (eq 7). Complex **4** displays the expected molecular mirror



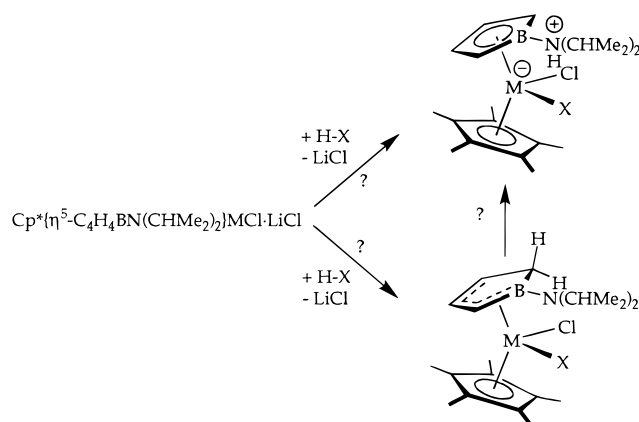
plane of symmetry in both the ^1H and ^{13}C NMR spectra. The presence of a proton on the amino group is indicated by the characteristically broad peak at $\delta \sim 7.4$. Presumably, the reaction proceeds via initial σ -bond metathesis of the allyl ligand by 1 equiv of the acetylene, followed by heterolysis of the other equiv to lead to the observed product.

While we were carrying out these studies of H–X bond heterolysis, Herberich and co-workers reported a reaction between iron phenylborole complexes and methyl iodide, in which the 2,5-positions of the borole were alkylated (eq 8).¹¹ Their results, along with



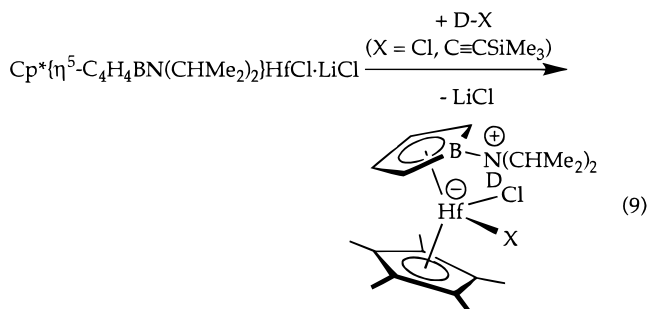
similar results in our group that arose during our investigations of the reactions of alkyl iodides with the group IV complexes,¹² suggested to us the worrying possibility that the H–X heterolytic reactions might

(11) Herberich, G. E.; Carstensen, T.; Koffer, D. P. J.; Klaff, N.; Boesse, R.; Hyla-Kryspin, I.; Gleiter, R.; Stephan, M.; Meth, H.; Zenneck, U. *Organometallics* **1994**, *13*, 619.

Scheme 1

proceed via initial protonation of the 2,5-positions rather than via direct involvement of the amino group. Such a reaction, followed by an intra- or intermolecular proton transfer from carbon to nitrogen could then account for the products we observe (Scheme 1).

To test whether this mechanism might be operating, we undertook control experiments using the deuterium-labeled substrates DCl and (trimethylsilyl)acetylene- d_1 (eq 9). In both cases, in the ^1H NMR of the d_1



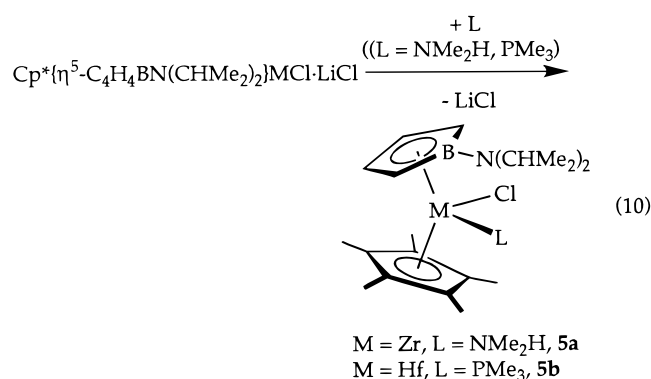
product, the peak assigned to the amino proton is completely absent and the integrals of the peaks corresponding to the 2,5-positions of the borole are unchanged relative to what is found in the protio isotopomer. To verify that the deuterium label had been incorporated into the product, the ^2H NMR of Cp* $\{\eta^5\text{-C}_4\text{H}_4\text{BN}(\text{CHMe}_2)_2\}\text{HfCl}_2$ was undertaken. In this spectrum, only one peak was observed, a broad singlet at δ 6.4, verifying the incorporation of deuterium onto the nitrogen of the aminoborole ligand.

Of course, these control experiments do not exclude a mechanism involving stereospecific protonation/deprotonation, that is, one in which the same proton that is added to the 2,5-position of the borole migrates to the amino group. On the other hand a stereospecific *exo* addition of deuterium and stereospecific *endo* migration of protium from C-2 to nitrogen is excluded, as are mechanisms involving scrambling of the hydrogens in the intermediate. In this regard, Herberich and co-

(12) Reaction of methyl iodide with Cp* $\{\eta^5\text{-C}_4\text{H}_4\text{BN}(\text{CHMe}_2)_2\}\text{HfCl-LiCl}$ resulted in formation of a product whose X-ray structure clearly showed, despite a disorder problem, the methyl group bonded to the 2-position of the borole. Kiely, A. F.; Henling, L. M.; Bercaw, J. E. Unpublished results. Similarly, reaction of benzyl iodide with Cp* $\{\eta^5\text{-C}_4\text{H}_4\text{BN}(\text{CHMe}_2)_2\}\text{ZrCl-LiCl}$ results in a new species whose ^1H and ^{13}C NMR spectra are consistent with its formulation as the product resulting from alkylation of the 2-position of the borole. Pastor, A.; Bercaw, J. E. Unpublished results.

workers have shown that the iron borole complex shown in eq 8 incorporates deuterium into the 2,5-positions instantaneously upon contact with D₂O,¹¹ supporting the notion that facile deprotonation occurs from both faces (i.e., that protonation/deprotonation is not stereospecific). Thus, we feel that a mechanism involving direct protonation at the amino group is the more reasonable alternative.

In an effort to eliminate the problem of competitive formation of Cp* $\{\eta^5\text{-C}_4\text{H}_4\text{BN}(\text{CHMe}_2)_2\}\text{MCl}_2$ (M = Zr, Hf) in the heterolytic reactions, we have also prepared the lithium-halide-free complexes. Addition of 1 equiv of a donor ligand to the lithium chloride adducts does in fact result in the formation of the donor adducts with elimination of 1 equiv of lithium chloride (eq 10). The



deep blue dimethylamine complex **5a** and the blue-purple PMe₃ adduct **5b** have the vivid colors characteristic of 16-electron pentamethylcyclopentadienyl-aminoborole complexes. Although they also display ¹H NMR spectra characteristic of the expected C₁ symmetry, their spectra are somewhat different than those of the C₁-symmetric products of the heterolytic reactions above, since with no proton on the amino group, the methyl groups of the isopropyls are pairwise diastereotopic. Thus, fast rotation on the NMR time scale about the B–N bond causes the inner methyl group of one isopropyl with the outer methyl group of the other to be equivalent. The barrier to this B–N bond rotation was measured by variable-temperature NMR studies for complex **5b** and found to be 12.7 (1) kcal·mol⁻¹.¹³ This value is at the low end of the range for barriers to B–N bond rotation measured by Herberich for a series of late-transition-metal aminoborole complexes,¹⁴ consistent with our expectation that the degree of boron–nitrogen π bonding should be reduced in the early-transition-metal aminoborole complexes (vide supra).

Complex **5b** was recrystallized from hot heptane, and the X-ray structure was determined for one of the crystals. A drawing of Cp* $\{\eta^5\text{-C}_4\text{H}_4\text{BN}(\text{CHMe}_2)_2\}\text{HfCl}(\text{PMe}_3)$ is shown in Figure 2, crystal data are listed in Table 1, and selected bond distances and angles are given in Table 3. The structure was disordered, due to the presence of two orientations of the amino group. This disorder was modeled as a mixture of the two

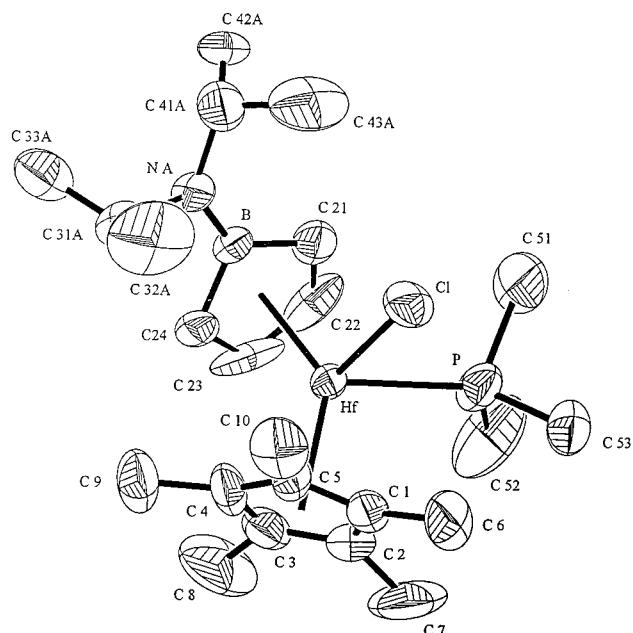


Figure 2. Drawing of Cp* $\{\eta^5\text{-C}_4\text{H}_4\text{BN}(\text{CHMe}_2)_2\}\text{HfCl}(\text{PMe}_3)$ (**5b**) (50% ellipsoids).

Table 3. Selected Distances (Å) and Angles (deg) for Cp* $\{\eta^5\text{-C}_4\text{H}_4\text{BN}(\text{CHMe}_2)_2\}\text{HfCl}(\text{PMe}_3)$ (5b**)**

Hf–Cp*	2.233	C22–C23	1.37(2)
Hf–Cl	2.425(2)	C23–C24	1.466(13)
Hf–P	2.740(3)	Hf–C21	2.487(8)
B–C21	1.525(11)	Hf–C22	2.453(9)
B–C24	1.525(10)	Hf–C23	2.349(9)
B–N(A)	1.49(2)	Hf–C24	2.383(7)
B–N(B)	1.39(5)	Hf–B	2.669(7)
C21–C22	1.368(13)		
Cl–Hf–P	83.6	C31–N(A)–B	119
Cp*–Hf–centroid _{B0}	134.4	C41–N(A)–B	124
C31–N(A)–C41	117	ΣN(B)	360

orientations (A and B) in the refinement with slightly different bond distances and angles for the amino group.

Addition of (trimethylsilyl)acetylene to **5b** results in the formation of a new species, which clearly no longer contains the isopropylamino group (¹H NMR). The new complex, **6**, still displays apparent C₁ symmetry by ¹H and ¹³C NMR spectroscopy. The shifts of the acetylide fragment in its ¹³C NMR spectrum are revealing. Although only one of the two acetylide peaks was located,¹⁵ no resonance was found downfield of the solvent (δ 128.4, benzene-*d*₆), suggesting the absence of an η¹-acetylide bonded to hafnium, since the α-carbons of such acetylides typically appear at δ > 150. Taken together, these results suggest that the acetylide group has migrated from hafnium to boron. Further evidence for this assignment, rather than an alternative involving direct displacement of diisopropylamine by phosphine, is found in the ³¹P NMR spectrum. Complex **6** displays only one resonance in this spectrum, a singlet at δ –9.36. The absence of any ¹¹B–³¹P coupling in the spectrum suggests that the phosphine is not bonded to boron.

Acceptable yields of complex **6** were obtained by the alternate pathway: reaction of complex **3** and trimethylphosphine (eq 11). A single crystal of **6** was obtained

(13) ΔG[‡] was calculated as follows. ΔG[‡] = 19.14T_c(10.32 + log(T_c/k_c)) J/mol, where T_c = coalescence temperature, k_c = πΔν/2, Δν = peak separation in ¹H NMR spectra of **3** at 230 K. ΔG[‡] is taken as an average of two values.

(14) Herberich, G. E.; Negele, M.; Ohst, H. *Chem. Ber.* **1991**, *124*, 25.

(15) The B–CCTMS resonance was not located, presumably due to quadrupolar broadening by the ¹¹B nuclei.

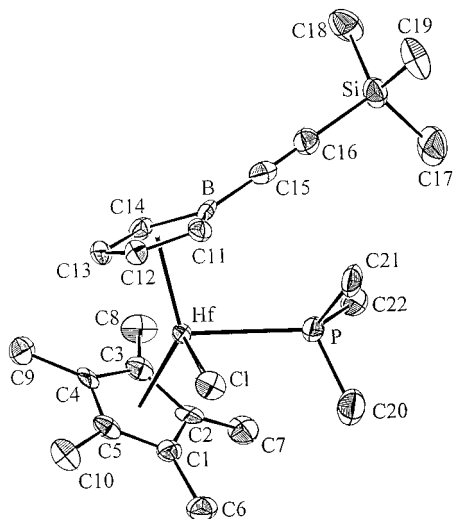
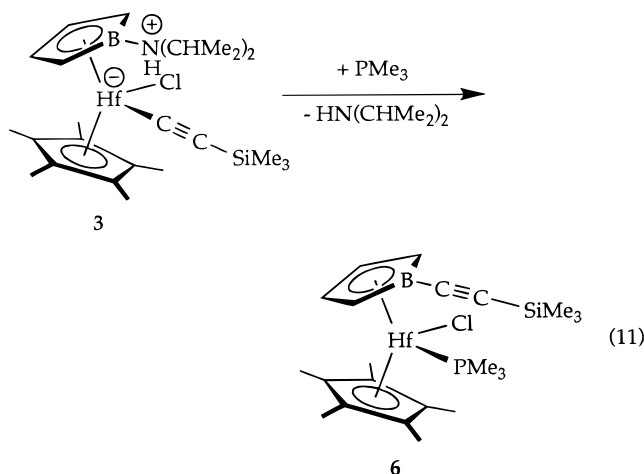


Figure 3. Drawing of $\text{Cp}^*(\eta^5\text{-C}_4\text{H}_4\text{B-C}\equiv\text{CSiMe}_3)\text{Hf}(\text{Cl})(\text{PMe}_3)$ (**6**) (50% ellipsoids).

Table 4. Selected Distances (Å) and Angles (deg) for $\text{Cp}^*(\eta^5\text{-C}_4\text{H}_4\text{B-C}\equiv\text{CSiMe}_3)\text{Hf}(\text{Cl})(\text{PMe}_3)$ (6**)**

Hf–Cp*	2.214	C13–C14	1.405(13)
Hf–Cl	2.434(2)	Si–C16	1.844(10)
Hf–P	2.732(3)	Hf–C11	2.519(10)
B–C11	1.507(15)	Hf–C12	2.441(9)
B–C14	1.513(14)	Hf–C13	2.379(9)
C11–C12	1.406(14)	Hf–C14	2.441(9)
C12–C13	1.416(13)	Hf–B	2.591(11)
Cl–Hf–P	82.7(1)	Si–C16–C15	177.3(9)
Cp*–Hf–centroid _{B₀}	133.0 (9)	C16–C15–B	175.9(10)



from a slowly cooled heptane solution. The crystals appeared to be unstable in the absence of the mother liquor. Thus, a crystal was placed in Paratone-N immediately upon its removal from the heptane solution, and the X-ray data collection was carried out at 160 K. An ORTEP diagram is shown in Figure 3, crystal data are given in Table 1, and selected bond distances and angles are given in Table 4. The crystal structure of the racemically twinned **6** verified the connectivity that is shown in eq 11.

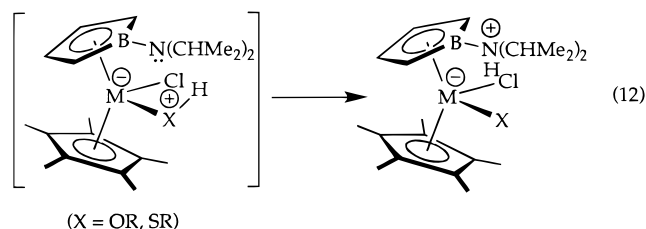
Preliminary kinetic data indicates that the mechanism for reaction 11 is not simple PMe_3 -induced acetylide migration. The rate appears to be independent of $[\text{PMe}_3]$. Although Herberich and co-workers have shown that the amino groups of dimethylaminoboroles are readily substituted when protonated, the independence

of the rate on $[\text{PMe}_3]$ suggests rate-limiting alkynyl migration with heterolysis of the B–N bond, followed by rapid capture by trimethylphosphine.¹⁶ Moreover, addition of excess diisopropylamine does not inhibit complete reaction to **6**, indicating that reaction 11, if reversible, lies far toward the products. Ashe and co-workers have recently reported an unusual annulation reaction of ethynes and boratabenzene complexes of zirconium for which a related alkenyl transfer from zirconium to boron was suggested.¹⁷

Conclusions

The combination of Lewis basic (nitrogen) and Lewis acidic sites (Zr or Hf) for these pentamethylcyclopentadienyl–aminoborole complexes of zirconium and hafnium work together in the heterolysis of even relatively weakly acidic H–X σ bonds of alcohols, thiols, and terminal acetylenes. Although the 2,5-carbon positions have been shown to also be quite nucleophilic in the reactions of aminoborole complexes of iron, deuterium-labeling experiments for these group 4 aminoborole complexes support direct deprotonation of hydrogen chloride and (trimethylsilyl)acetylene by nitrogen, with coordination of the conjugate base to zirconium or hafnium.

Displacement of coordinated lithium chloride is readily achieved using amine or phosphine ligands. These adducts react similarly with H–X bonds. The reactions of alcohols with $\text{Cp}^*\{\eta^5\text{-C}_4\text{H}_4\text{BN}(\text{CHMe}_2)_2\}\text{MCl}\cdot\text{LiCl}$ ($\text{M} = \text{Zr, Hf}$) appears to involve initial protonation of the amino nitrogen, followed by metathesis of neutral $\text{Cp}^*\{\eta^5\text{-C}_4\text{H}_4\text{BNH}(\text{CHMe}_2)_2\}\text{MCl}_2$ with LiOR . The mechanistic sequence leading to σ -bond heterolysis with $\text{Cp}^*\{\eta^5\text{-C}_4\text{H}_4\text{BN}(\text{CHMe}_2)_2\}\text{M}(\text{L})\text{Cl}$ ($\text{L} = \text{PMe}_3, \text{NHMe}_2$) is unclear at this stage. A likely alternative is displacement of L from the Lewis acidic metal center, with subsequent intramolecular proton transfer to nitrogen (eq 12). Reaction of (trimethylsilyl)acetylene may also



involve prior coordination via the sp -hybridized C–H σ -bonding electron pair, again followed by deprotonation.¹⁸

Thus far, we have been unable to effect heterolysis of sp^2 - or sp^3 -hybridized C–H bonds. It is not clear whether their lower reactivities are due to their higher $\text{p}K_a$'s or lower coordination abilities. Since both properties are inherently connected to the amount of s character in the C–H bonds, a clear distinction will be difficult.

(16) Our preliminary results do not discount stepwise amine loss and alkynyl migration.

(17) Ashe, A. J., III; Al-Ahmad, S.; Kampf, J. W.; Young, V. G., Jr. *Angew. Chem., Int. Ed. Engl.* **1997**, *36*, 2014.

(18) Prior coordination of the acetylene π bond(s) is also possible, but it is difficult to reconcile how such coordination would lie on the reaction pathway to the acetylide product.

Experimental Section

All manipulations were performed using glovebox and high-vacuum line techniques.¹⁹ Solvents were dried over Na/benzophenone ketyl and stored over Na/benzophenone ketyl (THF, ether) or titanocene²⁰ (toluene, petroleum ether, heptane). NMR solvents: benzene-*d*₆ was dried over LiAlH₄ and then over sodium metal; THF-*d*₈ was purified by vacuum transfer from Na/benzophenone ketyl. Argon was purified by passage over MnO on vermiculite and activated 4 Å molecular sieves. The complexes Cp*{η⁵-C₄H₄BN(CHMe₂)₂}MCl·LiCl (M = Zr, Hf) and Cp*{η⁵-C₄H₄BN(CHMe₂)₂}M(η³-C₃H₅) (M = Zr, Hf) were prepared according to the previously published procedures.¹⁰ CH₃OH (Fluka, anhydrous) and (trimethylsilyl)-acetylene were degassed and stored over activated molecular sieves. HCl (Matheson), DCl, D₂O (Cambridge Isotope Labs), and PMe₃ (Aldrich) were used as received. NMR spectra were carried out on a Bruker AM-500 spectrometer at 500 (¹H), 125.8 (¹³C), and 76.75 MHz (²H), a GE QE-300 spectrometer at 300 (¹H) and 75.5 MHz (¹³C), and a JEOL GX-400 spectrometer at 161.9 MHz (³¹P). All shifts reported for ¹H, ²H, and ¹³C NMR were referenced to the solvent. Shifts for ³¹P spectra were referenced to a H₃PO₄ standard. NMR-tube reactions were carried out using J. Young-type Teflon-valved NMR tubes purchased from Wilmad. Infrared spectra were recorded on a Perkin-Elmer 1600 Series FTIR. UV-vis spectra were recorded on a Hewlett-Packard 8452A spectrophotometer using a 1.0 mm path length, air-free cell. Elemental analyses were carried out by Mr. Fenton Harvey at Caltech. As past experience has shown, these group 4 borole compounds do not combust reliably and many elemental analyses proved to be irreproducible and inaccurate.

Cp*{η⁵-C₄H₄BNH(CHMe₂)₂}ZrCl(OC₆H₂-2,4,6-(CH₃)₃) (1a). A swivel frit assembly was charged with 0.42 g (0.86 mmol) of Cp*{η⁵-C₄H₄BN(CHMe₂)₂}ZrCl·LiCl and 0.12 g (0.87 mmol) of 2,4,6-trimethylphenol. Et₂O (25 mL) was condensed onto the solids at -78 °C. The reaction mixture was warmed to room temperature slowly. The color changed from purple to yellow and finally to green. Upon continued stirring, a white precipitate was formed. The reaction was stirred overnight and filtered to remove LiCl, and volatiles were removed under reduced pressure. The product was washed with 30 mL of petroleum ether and isolated by filtration, yielding 0.33 g (68%) of **1a** as a green solid. ¹H NMR (benzene-*d*₆, 500 MHz): δ 6.90 (s, br, 1H, aromatic ring), 6.87 (s, br, 1H, aromatic ring), 6.68 (s, br, 1H, N-H), 5.97 (m, H3), 5.95 (m, H4), 4.62 (m, H5), 4.05 (m, H2), 3.16 (pseudo sept, ³J_{HH} = 6.8 Hz, 1H, CH(CH₃)₂), 2.96 (pseudo sept, ³J_{HH} = 6.8 Hz, 1H, CH(CH₃)₂), 2.40 (s, 3H, CH₃), 2.30 (s, 3H, CH₃), 2.26 (s, 3H, CH₃), 2.02 (s, 15H, C₅(CH₃)₅), 0.92 (d, ³J_{HH} = 6.8 Hz, 3H, CH(CH₃)₂), 0.88 (d, ³J_{HH} = 6.8 Hz, 3H, CH(CH₃)₂), 0.87 (d, ³J_{HH} = 6.8 Hz, 3H, CH(CH₃)₂), 0.82 (d, ³J_{HH} = 6.8 Hz, 3H, CH(CH₃)₂). ¹³C{¹H} NMR (75.5 MHz, benzene-*d*₆): δ 129.20 (s, aromatic ring), 129.06 (s, aromatic ring), 119.0 (s, C₅(CH₃)₅), 118.0 (s, C3), 113.3 (s, C4), 102.7 (s, br, C2, C5), 96.1 (s, br, C2, C5), 50.9 (s, CH(CH₃)₂), 50.1 (s, CH(CH₃)₂), 20.5 (s, CH₃), 20.2 (s, CH₃), 20.0 (s, CH₃), 19.6 (s, CH₃), 19.4 (s, CH₃), 17.8 (s, CH₃), 11.8 (s, C₅(CH₃)₅). Anal. Calcd for C₂₉H₄₅BCINOZr: C, 62.07; H, 8.08; N, 2.50. Found: C, 62.72; H, 8.55; N, 2.65.

Cp*{η⁵-C₄H₄BNH(CHMe₂)₂}HfCl(OCH₃) (1b). A medium-sized fine-porosity swivel frit assembly with 100 mL flasks was loaded with 1.00 g (1.8 mmol) of Cp*{η⁵-C₄H₄BN(CHMe₂)₂}HfCl·LiCl in the drybox. The assembly was evacuated on the high-vacuum line, and 75 mL of toluene was added at -78 °C. An excess (20 equiv) of CH₃OH was added, and the solution changed from orange to yellow within 5 min. The

solution was stirred at -78 °C for 1.5 h, then allowed to warm to room temperature slowly over another hour. The solution was filtered, and the precipitate was washed 3 times with the volatile components of the filtrate. Volatiles were removed, and 75 mL of petroleum ether was added. Volatiles were removed in vacuo, and the assembly was taken into the drybox where the yellow oil was dissolved in a minimum amount of heptane and transferred into a 50 mL recrystallizing tube. After 12 h in the drybox freezer, a yellow solid had formed. The solid was isolated by filtration and stored in the glovebox freezer. Yield: 0.72 g, 73.8%. ¹H NMR (500 MHz, benzene-*d*₆): δ 6.56 (s, br, 1H, N-H), 5.84 (m, 2H overlapping, H3, H4), 4.94 (m, 1H, H2, H5), 4.17 (s, 3H, O-CH₃), 4.07 (m, 1H, H2, H5), 3.21 (pseudo sept, ³J_{HH} = 6.9 Hz, 1H, CH(CH₃)₂), 3.05 (pseudo sept, ³J_{HH} = 6.9 Hz, 1H, CH(CH₃)₂), 2.06 (s, 15H, C₅(CH₃)₅), 1.02 (d, ³J_{HH} = 6.9 Hz, 3H, CH(CH₃)₂), 0.95 (d, 6H overlapping, CH(CH₃)₂), 0.94 (d, ³J_{HH} = 6.9 Hz, 3H, CH(CH₃)₂). ¹³C{¹H} NMR (75.5 MHz, benzene-*d*₆): δ 117.2 (s, C₅(CH₃)₅), 114.3 (s, C3, C4), 111.0 (s, C3, C4), 97.6 (s, br, C2, C5), 93.3 (s, br, C2, C5), 61.1 (s, O-CH₃), 51.3 (s, CH((CH₃)₂)₂), 51.0 (s, CH((CH₃)₂)₂), 21.2 (s, CH((CH₃)₂)₂), 20.9 (s, CH((CH₃)₂)₂), 20.8 (s, CH((CH₃)₂)₂), 20.3 (s, CH((CH₃)₂)₂), 12.1 (s, C₅(CH₃)₅). Anal. Calcd for C₂₁H₃₇HfBNOCl: C, 46.40; H, 6.86; N, 2.58. Found: C, 46.00; H, 6.55; N, 2.39.

Cp*{η⁵-C₄H₄BNH(CHMe₂)₂}ZrCl(SC₆H₄-*p*-CH₃) (2a). A swivel frit assembly was charged with 0.4 g (0.85 mmol) of Cp*{η⁵-C₄H₄BN(CHMe₂)₂}ZrCl·LiCl and 0.1 g (0.80 mmol) of *p*-tolylthiol. Toluene (25 mL) was condensed onto the solids at -78 °C, and the mixture was stirred for 4 h at room temperature. The initially purple suspension turned yellow. Volatiles were removed under reduced pressure. The residue was redissolved in toluene and filtered to remove LiCl. Volatiles were removed, 20 mL of petroleum ether was condensed onto the residue, and **2a** was collected by filtration as a yellow solid (0.29 g, 62% yield). ¹H NMR (500 MHz, THF-*d*₈): δ 7.09 (d, ³J_{HH} = 7.9 Hz, 2H_o), 6.87 (d, ³J_{HH} = 7.9 Hz, 2H_m), 6.37 (br, 1H, N-H), 5.49 (m, H3), 5.17 (m, H4), 4.06 (m, H5), 3.78 (m, H2), 3.54 (pseudo sept, ³J_{HH} = 6.8 Hz, 1H, CH(CH₃)₂), 3.44 (pseudo sept, ³J_{HH} = 6.8 Hz, 1H, CH(CH₃)₂), 2.24 (s, 3H, phenyl CH₃), 1.93 (s, 15H, C₅(CH₃)₅), 1.30 (d, ³J_{HH} = 6.8 Hz, 3H, CH(CH₃)₂), 1.27 (d, ³J_{HH} = 6.8 Hz, 3H, CH(CH₃)₂), 1.24 (d, ³J_{HH} = 6.6 Hz, 3H, CH(CH₃)₂), 1.18 (d, ³J_{HH} = 6.4 Hz, 3H, CH(CH₃)₂). ¹³C{¹H} NMR (75.5 MHz, benzene-*d*₆): δ 143.1 (s, C_i), 133.6 (s, 2C_o), 132.6 (s, C_p), 128.0 (s, 2C_m), 118.8 (s, 5C, C₅(CH₃)₅), 117.0 (s, C3), 110.5 (s, C4), 103.2 (s, br, C2, C5), 98.7 (s, br, C2, C5), 51.0 (s, 1C, CH(CH₃)₂), 49.3 (s, 1C, CH(CH₃)₂), 20.4 (s, 2CH₃), 20.2 (s, CH₃), 19.7 (s, CH₃), 18.8 (s, 1CH₃), 11.6 (s, 5CH₃, C₅(CH₃)₅). Anal. Calcd for C₂₇H₄₁BCINSZr: C, 54.80; H, 6.90; N, 2.4. Found: C, 54.41; H, 6.37; N, 2.26.

Cp*{η⁵-C₄H₄BNH(CHMe₂)₂}MCl(SCH₃) (M = Zr, **2b; M = Hf, **2c**).** **Synthesis of 2b.** A 0.4 g (0.85 mmol) amount of Cp*{η⁵-C₄H₄BN(CHMe₂)₂}ZrCl·LiCl was suspended in 25 mL of toluene. The mixture was cooled to -78 °C, and a slight excess of CH₃SH (0.93 mmol) was condensed into the solution using a gas bulb (400 Torr, 42.5 mL gas bulb). The purple suspension became a cloudy orange solution and was stirred 2 h at room temperature. Volatiles were removed under reduced pressure. In the drybox, a swivel frit assembly was attached to the reaction flask. The residue was redissolved in petroleum ether, and LiCl was filtered off. The product was precipitated at -78 °C as a yellow microcrystalline solid. Recrystallization from a mixture of petroleum ether and Et₂O afforded orange-yellow crystals of **2b** (0.24 g, 60% yield). ¹H NMR (500 MHz, benzene-*d*₆): δ 7.5 (s, br, 1H, N-H), 5.94 (m, H3), 5.51 (m, H4), 4.78 (m, H5), 4.56 (m, H2), 3.67 (pseudo sept, ³J_{HH} = 6.8 Hz, 1H, CH(CH₃)₂), 2.98 (pseudo sept, ³J_{HH} = 6.8 Hz, 1H, CH(CH₃)₂), 2.65 (s, 3H, SCH₃), 2.00 (s, 15H, C₅(CH₃)₅), 1.05 (d, ³J_{HH} = 6.8 Hz, 3H, CH(CH₃)₂), 0.96 (d, ³J_{HH} = 6.9 Hz, 3H, CH(CH₃)₂), 0.93 (d, ³J_{HH} = 6.5 Hz, 3H, CH(CH₃)₂), 0.91 (d, ³J_{HH} = 6.7 Hz, 3H, CH(CH₃)₂). ¹³C{¹H} NMR (75.5

(19) Burger, B. J.; Bercaw, J. E. In *Experimental Organometallic Chemistry*; Wayda, A. L., Darensbourg, M. Y., Eds.; ACS Symposium Series 357; American Chemical Society, Washington, DC 1987.

(20) Marvich, R. H.; Brintzinger, H. H. *J. Am. Chem. Soc.* **1971**, *93*, 2046.

MHz, benzene- d_6): δ 118.9 (s, 5C, $C_5(CH_3)_5$), 114.8 (s, C3), 110.5 (s, C4), 104.2 (s, br, C2, C5), 100.4 (s, br, C2, C5), 52.4 (s, 1C, $CH(CH_3)_2$), 48.5 (s, 1C, $CH(CH_3)_2$), 21.0 (s, 2 CH_3), 19.9 (s, CH_3), 18.3 (s, CH_3), 11.9 (s, 5 CH_3 , $C_5(CH_3)_5$). Anal. Calcd for $C_{21}H_{37}BClNSZr$: C, 53.32; H, 7.88; N, 2.96. Found: C, 53.19; H, 8.21; N, 3.38.

Cp* $\{\eta^5-C_4H_4BNH(CHMe_2)_2\}HfCl(C\equiv CSiMe_3)$ (3). A medium-sized fine-porosity frit assembly with 100 mL flasks was loaded with 2.00 g (3.6 mmol) of $Cp^*\{\eta^5-C_4H_4BN(CHMe_2)_2\}HfCl\cdot LiCl$ in the drybox. The apparatus was evacuated on the high-vacuum line, and 40 mL of toluene was condensed onto the solid to give a deep orange solution. Then 1.1 equiv of (trimethylsilyl)acetylene was added via a 104 mL gas bulb (4×176 Torr). The solution was heated to 80 °C in an oil bath for 75 min, slowly changing from orange to yellow in color. The solution was cooled to room temperature, and the LiCl precipitate was allowed to settle for 30 min and filtered off. Volatiles were removed, and then 30 mL of petroleum ether was added and removed in vacuo to facilitate removal of residual toluene. The crude product was recrystallized from 40 mL of hot heptane, yielding 1.49 g (67.7%) of $Cp^*\{\eta^5-C_4H_4BNH(CHMe_2)_2\}HfCl(C\equiv CSiMe_3)$ as yellow-orange crystals. 1H NMR (500 MHz, benzene- d_6): δ 7.47 (s, br, 1H, N–H), 5.90 (m, 1H, H3, H4), 5.61 (m, 1H, H3, H4), 5.15 (m, 1H, H2, H5), 3.85 (m, 1H, H2, H5), 3.55 (pseudo sept, $^3J_{HH} = 6.8$ Hz, 1H, $CH(CH_3)_2$), 3.04 (pseudo sept, $^3J_{HH} = 6.7$ Hz, 1H, $CH(CH_3)_2$), 2.10 (s, 15H, $C_5(CH_3)_5$), 1.06 (m, 6H, $CH(CH_3)_2$), 0.98 (m, 6H, $CH(CH_3)_2$), 0.23 (s, 9H, $CCSi(CH_3)_3$). ^{13}C NMR (125.8 MHz, benzene- d_6): δ 183.0 (s, $CCSiMe_3$), 131.6 (s, $CCSiMe_3$), 118.22 (s, $C_5(CH_3)_5$), 114.1 (d, $^1J_{CH} = 160$ Hz, C3, C4), 110.4 (d, $^1J_{CH} = 163$ Hz, C3, C4), 106.5 (d, br, C2, C5), 96.3 (d, br, C2, C5), 52.4 (d, $^1J_{CH} = 142$ Hz, $CH(CH_3)_2$), 50.6 (d, $^1J_{CH} = 140$ Hz, $CH(CH_3)_2$), 20.0–21.5 (overlapping, 2 $CH(CH_3)_2$), 12.9 (q, $^1J_{CH} = 125$ Hz, $C_5(CH_3)_5$), 1.37 (q, $^1J_{CH} = 119$ Hz, $CCSi(CH_3)_3$). IR (Nujol): 2010 cm^{-1} ($\nu(CC)$). Anal. Calcd for $C_{25}H_{43}BClHfN$: Si: C, 49.21; H, 7.05; N, 2.29. Found: C, 48.98; H, 7.17; N, 2.22.

Cp* $\{\eta^5-C_4H_4BND(CHMe_2)_2\}HfCl(C\equiv CSiMe_3)$ (3- d_1). Trimethylsilylacetylene-1- d_1 was prepared by treatment of $LiC\equiv CSiMe_3$ with D_2O and distillation of the acetylene from the reaction solvent (toluene). Preparation of $Cp^*\{\eta^5-C_4H_4BND(CHMe_2)_2\}HfCl(C\equiv CSiMe_3)$ was analogous to that of the protio isotopomer. 1H NMR (300 MHz, benzene- d_6): δ 5.90 (m, 1H, H3, H4), 5.61 (m, 1H, H3, H4), 5.15 (m, 1H, H2, H5), 3.85 (m, 1H, H2, H5), 3.55 (pseudo sept, $^3J_{HH} = 7$ Hz, 1H, $CH(CH_3)_2$), 3.04 (pseudo sept, $^3J_{HH} = 7$ Hz, 1H, $CH(CH_3)_2$), 2.10 (s, 15H, $C_5(CH_3)_5$), 1.06 (d, $^3J_{HH} = 7$ Hz, 3H, $CH(CH_3)_2$), 1.05 (d, $^3J_{HH} = 7$ Hz, 3H, $CH(CH_3)_2$), 0.98 (d, $^3J_{HH} = 7$ Hz, 3H, $CH(CH_3)_2$), 0.97 (d, $^3J_{HH} = 7$ Hz, 3H, $CH(CH_3)_2$), 0.23 (s, 9H, $C\equiv CSi(CH_3)_3$).

Cp* $\{\eta^5-C_4H_4BNH(CHMe_2)_2\}Hf(C\equiv CSiMe_3)_2$ (4). A J. Young-type NMR tube was charged with 50 mg (0.097 mmol) of $Cp^*\{\eta^5-C_4H_4BN(CHMe_2)_2\}Hf(\eta^3-C_3H_5)$ and 0.75 mL of benzene- d_6 . On the vacuum line, 2.0 equiv of (trimethylsilyl)acetylene was added via condensation from a calibrated gas bulb. Upon thawing, the solution changed color from blue to orange-yellow. Volatiles were evaporated, and fresh benzene- d_6 was added (0.75 mL). The reaction was complete in 6 h. 1H NMR (300 MHz, benzene- d_6): δ 7.4 (br, 1H, N–H), 5.57 (m, 2H, H3, H4), 4.84 (m, 2H, H2, H5), 3.42 (pseudo sept, $^3J_{HH} = 6.6$ Hz, 2H, $CH(CH_3)_2$), 2.17 (s, 15H, $C_5(CH_3)_5$), 1.14 (d, $^3J_{HH} = 6.6$ Hz, 6H, $CH(CH_3)_2$), 1.02 (d, $^3J_{HH} = 6.6$ Hz, 6H, $CH(CH_3)_2$), 0.22 (s, 18H, $CC(Si(CH_3)_3)_2$). $^{13}C\{^1H\}$ NMR (75.5 MHz, benzene- d_6): δ 183.54 (s, $CC(Si(CH_3)_3)_2$), 128.92 (s, $CC(Si(CH_3)_3)_2$), 117.1 (s, $C_5(CH_3)_5$), 109.96 (s, C3, C4), 102 (br, C2, C5), 50.9 (s, $CH(CH_3)_2$), 20.76 (s, $CH(CH_3)_2$), 20.68 (s, $CH(CH_3)_2$), 12.74 (s, $C_5(CH_3)_5$), 0.937 (s, $CC(Si(CH_3)_3)_2$). IR (Nujol): 2025 (w, $\nu(CC)$) 2007 cm^{-1} (m, $\nu(C\equiv C)$).

Cp* $\{\eta^5-C_4H_4BND(CHMe_2)_2\}HfCl_2$. A swivel frit assembly was charged with 250 mg of $Cp^*\{\eta^5-C_4H_4BN(CHMe_2)_2\}HfCl\cdot LiCl$ (0.45 mmol). THF (20 mL) was condensed in at –78 °C.

The vacuum manifold was exposed to D_2O vapor from hot D_2O (5 mL) for 5 min to exchange acidic sites on the silica. The manifold was evacuated for 5 min. to remove the vapor. DCl (1 equiv) was added by gas bulb to the solution. Upon warming, the solution changed from red to yellow in color. Work up and recrystallization was as for the HCl analogue, with 90 mg (37%) isolated. 1H NMR (300 MHz, benzene- d_6): δ 5.90 (m, 2H, H3, H4), 4.75 (m, 2H, H2, H5), 3.25 (sept, $^3J_{HH} = 7$ Hz, 2H, $2CH(CH_3)_2$), 2.15 (s, 15H, $C_5(CH_3)_5$), 0.97 (d, $^3J_{HH} = 7$ Hz, 6H, $CH(CH_3)_2$), 0.92 (d, $^3J_{HH} = 7$ Hz, 6H, $CH(CH_3)_2$). 2H NMR (76.75 MHz, cyclohexane- d_{12}): δ 6.4 (br, 1D, $ND(CH_3)_2$).

Cp* $\{\eta^5-C_4H_4BN(CHMe_2)_2\}Zr(Cl)(NHMe_2)$ (5a). A 50 mL round-bottom flask was loaded with 0.43 g (0.92 mmol) of $Cp^*\{\eta^5-C_4H_4BN(CHMe_2)_2\}ZrCl\cdot LiCl$ and fitted with a vacuum adapter. The solid was slurried in toluene (25 mL) at –78 °C. Me_2NH (2.5 equiv) was vacuum transferred onto the suspension. The reaction mixture turned blue and was allowed to warm to room temperature slowly and stir overnight. Volatiles were removed, and a swivel frit assembly was attached to the flask in the drybox. The residue was extracted with 25 mL of toluene, and LiCl was removed by filtration. Volatiles were removed, and a blue solid was obtained. The resulting product was washed once with petroleum ether and dried in vacuo, yielding 0.28 g of **5a** as a blue solid. The compound can be recrystallized from hot heptane. 1H NMR (500 MHz, benzene- d_6 , 298 K): δ 5.84 (pseudo sept, $^3J_{HH} = 6.0$ Hz, 1H, $NH(CH_3)_2$), 5.76 (m, H3), 5.46 (m, H4), 5.28 (m, H5), 3.47 (br, 2H, $CH(CH_3)_2$), 3.41 (m, H2), 2.19 (s, br, 3H, $NHCH_3$), 1.79 (s, 15H, $C_5(CH_3)_5$), 1.76 (br, 3H, $NHCH_3$), 1.38 (br, 6H, $CH(CH_3)_2$), 1.16 (br, 6H, $CH(CH_3)_2$). 1H NMR (500 MHz, toluene- d_8 , 245 K): δ 6.0 (s, br, 1H, N–H), 5.77 (m, H3), 5.40 (m, H4), 5.32 (m, H5), 3.43 (m, 2H, $2CH(CH_3)_2$), 3.29 (m, H2), 2.17 (d, $^3J_{HH} = 6.0$ Hz, 3H, $NHCH_3$), 1.75 (s, 15H, $C_5(CH_3)_5$), 1.66 (d, $^3J_{HH} = 6.0$ Hz, 3H, $NHCH_3$), 1.45 (d, $^3J_{HH} = 6.4$ Hz, 3H, $CH(CH_3)_2$), 1.40 (d, $^3J_{HH} = 6.7$ Hz, 3H, $CH(CH_3)_2$), 1.18 (d, $^3J_{HH} = 6.4$ Hz, 3H, $CH(CH_3)_2$), 1.14 (d, $^3J_{HH} = 6.6$ Hz, 3H, $CH(CH_3)_2$). $^{13}C\{^1H\}$ NMR (75.5 MHz, benzene- d_6): δ 122.6 (s, C4), 119.8 (s, 5C, $C_5(CH_3)_5$), 116.7 (s, C3), 107.0 (s, br, C2, C5), 95.0 (s, br, C2, C5), 49.7 (s, 1C, $CH(CH_3)_2$), 45.9 (s, 1C, $CH(CH_3)_2$), 42.2 (s, NCH_3), 39.1 (s, NCH_3), 23.6 (s, 4C, CH_3), two small broad signals at 22.8 and 24.4, 11.9 (s, 5 CH_3 , $C_5(CH_3)_5$). Anal. Calcd for $C_{22}H_{40}BClN_2Zr$: C, 56.22; H, 8.58; N, 5.96. Found: C, 55.97; H, 8.27; N, 5.89.

Cp* $\{\eta^5-C_4H_4BN(CHMe_2)_2\}Hf(Cl)(PMe_3)$ (5b). A large fine-porosity frit assembly with 250 mL flasks was loaded with 2.00 g (3.6 mmol) of $Cp^*\{\eta^5-C_4H_4BN(CHMe_2)_2\}HfCl\cdot LiCl$ in the drybox. The assembly was evacuated on the high-vacuum line, and then 100 mL of toluene was condensed onto the solid at –78 °C. PMe_3 (1.0 equiv) was added via a calibrated gas bulb (104 mL gas bulb, 641.5 Torr), and the solution was stirred for 3 h, slowly warming to room temperature from –78 °C. Then the LiCl was filtered away from the purple solution and volatiles were removed in vacuo. Petroleum ether (100 mL) was condensed in and removed, and then another 100 mL of petroleum ether was added to give a purple precipitate. The solid was collected by filtration, volatiles were removed, and the apparatus was taken into the drybox. The purple solid was collected and weighed into a vial and stored in the drybox freezer. Yield: 1.63 g (76.9%). 1H NMR (500 MHz, benzene- d_6): δ 5.80 (m, 1H, H3, H4), 4.59 (m, 1H, H3, H4), 4.52 (m, 1H, H2, H5), 4.42 (m, 1H, H2, H5), 3.77 (m, br, 2H, $CH(CH_3)_2$), 1.89 (s, 15H, $C_5(CH_3)_5$), 1.43 (d, $^3J_{HH} = 6.7$ Hz, 6H, $CH(CH_3)_2$), 1.37 (d, $^3J_{HH} = 6.7$ Hz, 6H, $CH(CH_3)_2$), 0.84 (d, $^2J_{PH} = 7.15$ Hz, 9H, $P(CH_3)_3$). $^{13}C\{^1H\}$ NMR (125.8 MHz, C_6D_6): δ 121.2 (s, $C_5(CH_3)_5$), 117.9 (s, C3, C4), 111.2 (s, C3, C4), 96.7 (s, br, C2, C5), 94.9 (s, br, C2, C5), 47.9 (s, $CH((CH_3)_2)_2$), 24.3 (s, $CH((CH_3)_2)_2$), 24.2 (s, $CH((CH_3)_2)_2$), 16.4 (d, $^1J_{PC} = 20.4$ Hz, $P(CH_3)_3$), 12.8 (s, $C_5(CH_3)_5$). $^{31}P\{^1H\}$ NMR (161.9 MHz, benzene- d_6): δ –11.93 (s, $P(CH_3)_3$). UV–vis (toluene): $\lambda_{max} = 572$ nm ($\epsilon = 830$ $M^{-1} cm^{-1}$). Anal. Calcd for $C_{23}H_{42}HfBNP$: Cl:

C, 46.96; H, 7.20; N, 2.36. Found: C, 42.27, 46.47, 41.28, 48.32; H, 6.75, 7.27, 5.73, 6.47; N, 2.02, 2.14, 2.32, 2.30.

Cp* $\{\eta^5\text{-C}_4\text{H}_4\text{B-C}\equiv\text{CSiMe}_3\}\text{HfCl(PMe}_3\text{)}$ (6**).** A large fine-porosity frit assembly with 250 mL flasks was loaded with 1.00 g (1.64 mmol) of Cp* $\{\eta^5\text{-C}_4\text{H}_4\text{BNH(CHMe}_2\text{)}_2\}\text{HfCl(C}\equiv\text{CSiMe}_3\text{)}$ (**3**) in the drybox. The assembly was evacuated on the high-vacuum line, and then 200 mL of toluene was condensed onto the solid at -78°C . PMe₃ (1.1 equiv) was added via a calibrated gas bulb (104 mL gas bulb, 321 Torr), and the solution was stirred, slowly warming to room temperature from -78°C . After 2 weeks of stirring at room temperature, the volatiles were removed in vacuo. Then 100 mL of petroleum ether was condensed onto the residue and removed, and another 100 mL portion petroleum ether was added to give an orange precipitate. The solid was collected by cold filtration, the volatiles were removed, and the apparatus was taken into the drybox. The orange solid was collected and weighed into a vial and stored in the drybox freezer. Yield: 0.405 g (42.2%). Recrystallization was possible from a slowly cooled heptane solution. ¹H NMR (500 MHz, benzene-*d*₆): δ 6.11 (m, 1H, H3, H4), 6.07 (m, 1H, H3, H4), 5.79 (m, 1H, H2, H5), 5.34 (m, 1H, H2, H5), 1.79 (s, 15H, C₅(CH₃)₅), 1.29 (d, ²J_{PH} = 6.2 Hz), 0.22 (s, 9H, CCSI(CH₃)₃). ¹³C{¹H} NMR (125.8 MHz, benzene-*d*₆): δ 125.79 (s, C3, C4), 119.90 (s, C₅(CH₃)₅), 117.78 (s, br, C2, C5), 116.07 (s, C3, C4), 115.02 (s, br, C2, C5), 111.14 (s, B-CCSi(CH₃)₃), 16.96 (d, ¹J_{PC} = 23.19 Hz, P(CH₃)₃), 12.45 (s, C₅(CH₃)₅), 1.00 (s, B-CCSi(CH₃)₃; B-CCSi(CH₃)₃ not located). ³¹P{¹H} NMR (161.9 MHz, benzene-*d*₆): δ -9.64 (s, P(CH₃)₃). IR (Nujol): 2102 cm⁻¹ (ν (CC)). UV-vis (toluene): λ_{max} = 486 nm (ϵ = 1354 M⁻¹ cm⁻¹).

X-ray Crystal Structure Determinations. For **3** and **5b**, a suitable crystal was mounted with grease in a capillary tube and optically centered on the diffractometer. Crystals of **6** were unstable in the absence of the mother liquor. Therefore, crystals of **6** were placed in Paratone-N immediately upon removal from the mother liquor, and a suitable crystal was mounted on a glass fiber with Paratone-N and optically centered on the diffractometer in a cold stream at 160 K. Data for **3** and **5b** were collected at room temperature; data for **6** were collected at 160 K. For each compound, the unit cells were determined from the setting angles of 25 reflections. For **3** and **6**, two equiv sets of data were collected. The crystallographic data are summarized in Table 1. Lorentz and

polarization factors were applied, and the intensities were corrected for decay (based on 3 standards) and absorption (based on γ -scans of 6 reflections). The data were merged in the appropriate point group using CRYM²¹ programs. Weights w were calculated as $1/s^2(F_o^2)$; variances ($s^2(F_o^2)$) were derived from counting statistics plus an additional term, $(0.014I)^2$; variances of the merged data were obtained by propagation of error plus another additional term, $(0.014\bar{I})^2$.

Each structure was solved using SHELXS-86²² by direct methods. Each was refined by full-matrix least squares using SHELXL-93²³ for **5b** and CRYM²¹ for **3** and **6**. Hydrogen atoms were included in the refinements at calculated positions. For **5b**, disorder was observed and modeled in the borole ligands. Crystals of **6** were enantiomerically twinned with a 1:1 ratio of the twin components. The data were merged in point group *mmm*, and the structure factors were calculated with a fixed 1:1 ratio of Friedel mates.

Complete listing of fractional coordinates, displacement parameters, bond distances and angles, and structure factors for **3**, **5b**, and **6** have been deposited at the Cambridge Crystallographic Data Centre, 12 Union Road, Cambridge, CB2 1EZ, U.K., and copies can be obtained on request free of charge.

Acknowledgment. This work has been supported by the National Science Foundation (Grant No. CHE-9506413). A.P. thanks the Ministerio de Educación y Ciencia of Spain for a postdoctoral fellowship. The authors wish to thank Timothy Herzog for his help in obtaining the ²H NMR spectra and David Lynn for his help in obtaining the ³¹P NMR spectra.

Supporting Information Available: Tables giving positional and thermal parameters and bond distances and angles for **3**, **5b**, and **6** (17 pages). Ordering information is given on any current masthead page.

OM9709345

(21) Duchamp, D. J. The CRYM Crystallographic Computing System. American Crystallography Association Meeting, Bozeman, Montana, 1964; Paper B14, pp 29–30.

(22) Sheldrick, G. M. *Acta Crystallogr.* **1990**, *A46*, 467.

(23) Sheldrick, G. M. *Program for Structural Refinement*; University of Göttingen: Göttingen, Germany, 1993.